ICAS-98-7,4,2

A98-31700

CONICAL EULER EQUATIONS' SOLUTION BASED ON THE UNSTRUCTURED GRID AND ITS APPLICATION TO A VORTICAL FLOW OVER A HIGHLY SWEPT DELTA WING

Ping-Hong Yao and Etsuo Morishita

Department of Aeronautics and Astronautics
Graduate School of Engineering
The University of Tokyo
7-3-1, Hongo, Bunkyo-ku, Tokyo 113-8656, Japan

Abstract

The supersonic flow over highly swept delta wings was analyzed by using conical flow equations. Numerical solutions for Euler equations were obtained by introducing the artificial damping terms to suppress the numerical oscillations due to shock waves. The authors attempted to develop the conical Navier-Stokes equations whose viscous terms were modified as in the conical Euler equations in order to replace the artificial damping terms. First, preliminary numerical studies were done based on simple rectangular grids by utilizing the spreadsheet cells and their iteration functions instead of depending on the computer programs. An unstructured example is also being anlyzed. The numerical results were compared to the supersonic experimental data of swept delta wings with subsonic and supersonic leading edges.

Nomenclature

b	: span
c	: chord
Cp	: pressure coefficient
E, F, G	: flux vector
E_v, F_v, G_v	: viscous flux vector
M	: Mach number
p	: static pressure
Q	: vector of conservative flow quantities
Pr	: Prandtl number
Re	: Reynolds number
t	: time
T	: temperature
u,v,w	: velocity components in x-,y-,z-direction
x,y,z	: coordinates
α	: angle of attack
γ	: specific heat ratio
Λ	: sweep-back angle
ρ	: density
τ	: shearing stress

Introduction

The flow over delta wings was numerically examined based on the assumption of the conical flow. Conical Euler equations have been used to solve this type of flow by researchers[1][2]. The authors attempted to solve the above problems first by using the same technique based on an unstructured grid. In other studies, artificial viscous damping terms were used to avoid numerical oscillations[2]; in this study, therefore, the artificial damping terms were replaced by real viscous terms which were modified based on the assumption of a conical flow. This assumption implies that the flow

21st ICAS Congress
13-18 September 1998
Melbourne, Australia

on a ray from the apex of the delta wing has the same physical properties. In general, similarity coordinate is used to express the conical flow field so that the flow variation in the direction of the main stream is not taken into account and only the span-wise and the normal-to-wing directions are considered. The above problem thereby becomes a two-dimensional one that can be easily analyzed while the solutions keep the three-dimensional information.

The conical Euler equation, which was actually modified into the conical Navier-Stokes equation, was first solved on simple rectangular grids in order to test the validity of the assumption in the equations. CFD(Computational Fluid Dynamics) is normally anlyzed via computer language; this process, however, is sometimes time consuming. In previous studies, the authors found that the spreadsheet software is very useful for fluid dynamic numerical simulations[3],[4], because the spreadsheet has build-in cells which correspond to the grids in CFD, and because of its iteration functions which can specify the number of iterations and the tolerance needed to terminate the computation. The spreadsheet also has its own graphics software, which facilitates the presentation of the results. The conical flow equations were discretized in finite differential forms and were put into the cells of a spreadsheet, and the boundary conditions in finite difference forms were also written in boundary cells, and the iteration in the cells was then begun. After the computational convergence was examined, graphical output was produced by selecting the relevant area.

The pressure data for the "Lee-Side Flow over Delta Wings at Supersonic Speeds" (NASA TP 2430, 1985[5]) are available and the same conditions were used for computation. Due to the preliminary nature of the calculation, flat plate delta wings with zero thickness were used. Both subsonic and supersonic leading edges were studied. The Mach number range was from 1.7 to 2.8 and the Reynolds number was 2 million based on the span of the delta wing. The half-span of the delta wings was calculated due to the symmetry.

An unstructured example based on Delaunay triangulations using the conical Euler equations is also being studied.

Governing Equations

Conical Flow Equations

The 3-D Navier-Stokes equations are given by

$$\frac{\partial \mathbf{Q}}{\partial t}+\frac{\partial \mathbf{E}}{\partial x}+\frac{\partial \mathbf{F}}{\partial y}+\frac{\partial \mathbf{G}}{\partial z}=\frac{\partial \mathbf{E}_v}{\partial x}+\frac{\partial \mathbf{F}_v}{\partial y}+\frac{\partial \mathbf{G}_v}{\partial z} \quad (1)$$

Eq.(1) is non-dimensionalized by the principal variables[6]. The conical flow assumption is as follows[2]:

$$\bar{x} \equiv x, \quad \bar{y} \equiv \frac{y}{x}, \quad \bar{z} \equiv \frac{z}{x} \quad (2)$$

Note that x, y and z in Eq.(2) are already non-dimensional. When Eq.(2) is applied to Eq.(1) and the bar in Eq.(2) is omitted for the sake of simplicity, the following equation is obtained:

$$\frac{\partial \mathbf{Q}}{\partial t}+\frac{\partial(\mathbf{F}-y\mathbf{E})}{\partial y}+\frac{\partial(\mathbf{G}-z\mathbf{E})}{\partial z}+2\mathbf{E} = \frac{\partial(\mathbf{F}_v-y\mathbf{E}_v)}{\partial y}+\frac{\partial(\mathbf{G}_v-z\mathbf{E}_v)}{\partial z}+2\mathbf{E}_v \quad (3)$$

It is assumed that the x-derivative is zero in the conical flow assumption, and Eq.(3) is examined at cross-section $x=1$. The right-hand-side terms were actually analyzed in non-conservative forms in the numerical procedure:

$$r.h.s.Eq.(3) = -y\frac{\partial \mathbf{E}_v}{\partial y}-z\frac{\partial \mathbf{E}_v}{\partial z}+\frac{\partial \mathbf{F}_v}{\partial y}+\frac{\partial \mathbf{G}_v}{\partial z} \quad (4)$$

When the right-hand-side of Eq.(3) is not taken into account, this is a conical Euler equation.

Conical Flow Assumption in Viscous Terms

One of the elements of the viscous flux terms in Eq.(3) is (for example) given by

$$\tau_{xy}=\frac{1}{Re}\left(\frac{\partial v}{\partial x}+\frac{\partial u}{\partial y}\right) \quad (5)$$

If the conical flow assumption in Eq.(2) is applied even to the viscous terms, Eq.(5) becomes

$$\tau_{xy}=\frac{1}{Re}\left(\frac{\partial v}{\partial x}+\frac{\partial u}{\partial y}\right)=\frac{1}{Re}\left(-y\frac{\partial v}{\partial y}-z\frac{v}{\partial z}+\frac{\partial u}{\partial y}\right) \quad (6)$$

where the physical properties of the flow are

assumed to be constant for the sake of simplicity. The remaining viscous terms were examined in the same manner.

Computational Procedure

Finite Difference

First, the authors attempted to evaluate the validity of the conical flow assumption, and Eq.(3) was discretized by the simple FTCS method. In addition, classical rectangular grids 20 x 20 in y-(span-wise) and z-(normal-to-wing) directions were used. The computational domain is

$$0 \le y \le b, \quad -1 \le z \le 1 \tag{7}$$

where y and z values are normalized via the chord c of the delta wing and, therefore,

$$b = 2\tan(\frac{\pi}{2} - \Lambda) \tag{8}$$

The cross-section of the delta wing is modeled as a flat plate and is located in the computational space as follows:

$$0 \le y \le \tan(\frac{\pi}{2} - \Lambda), \qquad z = 0 \tag{9}$$

The finite difference mesh size then becomes

$$\Delta y = \frac{\tan(\frac{\pi}{2} - \Lambda)}{10}, \quad \Delta z = 0.1 \tag{10}$$

(This mesh size is too coarse for a flow class at Re =2 x 10^6 ; therefore, the authors attempted to obtain an overview of the flow field.)

Computing by Spreadsheet - Spreadsheet Fluid Dynamics(SFD)[3],[4]

CFD usually involves lengthy program development and it sometimes becomes time consuming due to computer illiteracy and the complexity of the governing equations. The authors found that spreadsheets are very useful CFD tools, because the cells become natural grids and the iterative calculation between cells becomes possible. The authors call this technique Spreadsheet Fluid Dynamics (SFD) .

In this study potential flow in a camber with an inlet and an outlet is shown to make this process easier to understand. Figure 1(a) shows part of a spreadsheet and the flow region, which are rounded by colored cells. The value of the stream function is given on the colored boundary. One cell (e.g. B2 in Fig.1(a)) was selected, and the finite difference form of Laplace's equation was inputed, which becomes in a square grid as follows:

$$= (A2 + C2 + B1 + B3)/4 \tag{11}$$

Eq.(11) follows the spreadsheet format and it indicates that the value of cell B2 is the average of the neighboring four cells (which really the Laplacian means). The contents of cell B2 are copied into the other cells in the computational domain in Fig.1 The alphabet letters and numbers are automatically changed according to the location of the cell, and the spreadsheet is now ready to be computed. The iteration is then selected by specifying the number of iterations and the error tolerance when computing is terminated. Calculations were conducted and the stream function was readily obtained almost instantly by the graphics in the program(see Fig.1(b)). In order to accomplish the above, lengthy computer program lines and the specialized computer skills are unnecessary. The discretized governing equations and the boundary conditions are only needed.

Spreadsheet Fluid Dynamics was also applied to the problems in this study and a sample computational domain for the computation here is shown in Fig.2. This is actually part of the spreadsheet. The boundaries and the delta wing cross-section are colored

Computation via Spreadsheet Fluid Dynamics is explained as follows for the examples used in this study.

First, the physical properties of air, i.e., Prandtl number Pr and specific heat ratio γ , and the aerodynamic conditions like Mach number M and the Reynolds number Re were specified in the spreadsheet. Delta wing data, (i.e., the sweep-back angle and the angle of attack), were also specified. The computational conditions, (dy, dz and dt), were also given. A cell was selected in order to count the number of iterations.

Next, the initial and boundary conditions for the three velocity components and the three

thermodynamic properties (pressure p, density ρ and temperature T) were specified, and six 20x20 cell blocks were prepared for these values. One of the build-in features of Spreadsheet Fluid Dynamics is that it is not necessary to declare domains for variables.

The convection and viscous term cell blocks were then prepared. These correspond to the terms which are to be spatially differentiated. For the continuity equation, two 20x20 cell blocks and three 20x20 cell blocks were needed for the rest of the equations (three momentum and energy).

The discretized governing equations (Eq.3 with Eq.4) were written in the next four 20x20 cell blocks. These cell blocks gave the values for the next time step.

Six 20x20 cell blocks were used to store the new time level value of the three velocity components and the three thermodynamic properties.

Twelve 20x20 cell blocks were used to get space derivatives in the x-,y- and z- directions of the three velocity components (u, v and w) and static temperature T.

Finally, the viscous terms in the six 20x20 cell blocks and the viscous work and heat conduction terms in the three 20x20 cell blocks were obtaiend.

The spreadsheet automatically repeated the iteration and the computation was terminated when convergence was reached. It is significant that only one spreadsheet is necessary in the above process.

Initial and Boundary Conditions

The initial conditions were the same as the uniform flow conditions and the outer boundary values remained the same during computation. Along the symmetric plane, i.e. y=0, the zero-gradient condition was used. On a delta wing, the velocity components are all zero, and the temperature condition is either specified or adiabatic. The pressure on the delta wing is calculated from the momentum equation in the z-direction on the surface of the wing. The boundary layer assumption, (i.e., zero-normal pressure gradient) may be used for replacement.

Because a zero-thickness flat plate model was used for the delta wing, extra cell rows were prepared for the windward pressure value in the spreadsheet. It was important to use the average of the windward and the lee-side pressures when the derivatives in the y-direction were calculated at the leading edge of the delta wing. This was done in order to avoid unnecessary discontinuity.

Computational Conditions used to Compare the Experiments

The flat lee-side pressure data are available in NASA TP 2430[5] and the same computational conditions were used in our computation.

Sweep-back angle Λ 52.5deg., 67.5deg.
Mach number M 1.7, 2.0, 2.4, 2.8
Reynolds number Re 2×10^6 (based on the span)
Angle of attack α 4deg., 8 deg., 12deg., 16deg., 20deg.

The above calculations specified the temperature of the delta wing, which was the same as the uniform flow static temperature and was different from that in the experiment. However, the adiabatic wall conditions were examined, and the pressure difference was not significant between the constant temperature and the adiabatic conditions.

Comparisons were made to previous experimental data[5] and also to the linear theory for lee-side pressure[7] in the next section.

Computational Results and Comparison to Experiments NASA TP2430[5]

Figures 3 (a) ~ (e) show the calculated span-wise pressure distributions over a delta wing with a sweep-back angle of 67.5 degrees in a supersonic flow at M=1.7. The Reynolds number based one this span was 2×10^6. The angles of attack were 4, 8, 12, 16 and 20 degrees ((a),(b),(c),(d) and (e) respectively in Fig.3). Cpu denotes the lee-side and Cpl denotes the windward side. 'cal' shows the results from this study. The NASA experimental data on the lee-side of the delta wing[5] are also shown in Fig.3 (Cpu_exp). Linear theory[7] for the lee-side pressure is also included in Fig.3 (Cpu_th). Examples of subsonic leading edges are shown in Fig.3.

At most of the angles of attack, the authors' calculation did not predict the lee-side pressure near the leading edge; the coarse cells (grids) could be one of the causes. The NASA experiment was turbulent, while the simulation in this study had no turbulent

model. The size of the cells used here was very coarse to simulate the experimental vortical conditions. The leading edge vortex was not adequately simulated and the pressure peak was not reproduced in the above calculations. The calculated lee-side pressure near the axis of the wing was closer to that in the experiment at lower angles of attack. Linear theory, however, was even closer to that in the experiment as a whole for the conditions in Fig.3.

Figure 4 shows the results at M =2.4 for the same delta wing of Λ=67.5 degrees in Fig.3. Here, this lee-side pressure calculation was not acceptable compared to the NASA results at lower angles of attack. The lee-side pressure prediction by the above method, however, was closer to the NASA data at an angle of attack of 20 degrees. The reason for this is unclear. One possibility might be that the conical flow assumption in this study matches the experimental conditions at higher angles of attack.

Figure 5 shows the results for the same delta wing at M=2.8; this is the example of a supersonic leading edge. Again, the lee-side pressure prediction was not successful at lower angles of attack. At higher angles of attack (12, 16 and 20 degrees), the calculated lee-side pressure distributions again were in agreement with those in the experiments. The angle of attack of 16 degrees was the closest to that in the experiment.

Figure 6 shows the span-wise pressure distribution around a delta wing with a sweep-back angle of 52.5 degrees in a supersonic flow at M=2.8. This is the example of a supersonic leading edge with a moderate sweep-back angle. The experiments and numerical predictions were different from the linear theory for the supersonic leading edge. In addition, the predicted lee-side pressure distributions using the method in this study were similar to those in the NASA experiments at higher angles of attack(12, 16 and 20 degrees). At lower angles of attack, the prediction in this study were not similar to those in the experiments.

Although the windward side pressure distributions are also shown in Figs. 3-6, they were not compared to the experiment.

Conclusion

Conical flow equations were used to solve the flow around a highly swept delta wing in a supersonic flow. This study showed the results obtained form the conical Navier-Stokes equations that had been extended from similar conical Euler equations. Two delta wings with sweep-back angle of 67.5 and 52.5 degrees were studied in a supersonic flow with Mach numbers ranging from 1.7 to 2.8 at a Reynolds number of 2×10^6. The numerical solutions were obtained via spreadsheet (Spreadsheet Fluid Dynamics - SFD). The results were compared to the NASA experiments. It was found that, although the correct predictions at lower angles of attack were not possible, the predicted lee-side pressure distribution using this method agreed with the NASA data at higher angles of attack (around 12 – 20 degrees), especially when supersonic leading edge was calculated.

References

[1] Lee, E.M. and Batina, J.T., Conical Euler Solution for a Highly Swept Delta Wing Undergoing Wing-Rock Motion, NASA TM-102609, 1990.

[2] Lee, E.M. and Batina, J.T., Conical Euler Analysis and Active Roll Suppression for Unsteady Vortical Flows About Rolling Delta Wings, NASA TP-3259, 1993.

[3] Tanaka, H., Simple CFD by Spreadsheet, Graduation Thesis(in Japanese), Univ. Tokyo., Mar. 1998.

[4] Morishita, E. and Tanaka, H., Spreadsheet Fluid Dynamics(in Japanese), Proc. 29th Annual Meeting, JSASS, Tokyo, April, 1998, pp.58-59.

[5] Miller, D.S. and Wood, R.M., Lee-Side Flow Over Delta Wings at Supersonic Speeds, NASA TP 2430, June 1985.

[6] Hoffmann,K.A. and Chiang, S.T., Computational Fluid Dynamics for Engineers-Vol. II, Engineering Education System, Wichita, 1993, pp.25-28.

[7] Puckett, A.E., Supersonic Wave Drag of Thin Airfoils, Journal of the Aeronautical Sciences, Sept. 1946, pp.475-484.

	A	B	C	D	E	F	G	H	I	J	K
1	0	0	0	0	0	0	0	0	0	0	0
2	0.5										0
3	1										0
4	1										0
5	1										0
6	1										0
7	1										0
8	1										0
9	1										0
10	1										0
11	1										0.5
12	1										1
13	1	1	1	1	1	1	1	1	1	1	1

(a) Spreadsheet cells for computation

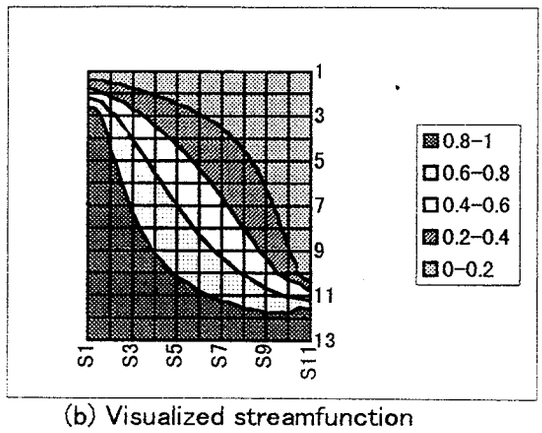

(b) Visualized streamfunction

Fig.1 Potential flow through a camber solved by spreadsheet

											Q											
rho	1	1	1	1	1	1	1	1	1	1	1	1	1	1	1	1	1	1	1	1	1	1
	0.9	0	0	0	0	0	0	0	0	0	0	0	0	0	0	0	0	0	0	0	0	1
	0.8	0	0	0	0	0	0	0	0	0	0	0	0	0	0	0	0	0	0	0	0	1
	0.7	0	0	0	0	0	0	0	0	0	0	0	0	0	0	0	0	0	0	0	0	1
	0.6	0	0	0	0	0	0	0	0	0	0	0	0	0	0	0	0	0	0	0	0	1
	0.5	0	0	0	0	0	0	0	0	0	0	0	0	0	0	0	0	0	0	0	0	1
	0.4	0	0	0	0	0	0	0	0	0	0	0	0	0	0	0	0	0	0	0	0	1
	0.3	0	0	0	0	0	0	0	0	0	0	0	0	0	0	0	0	0	0	0	0	1
	0.2	0	0	0	0	0	0	0	0	0	0	0	0	0	0	0	0	0	0	0	0	1
	0.1	0	0	0	0	0	0	0	0	0	0	0	0	0	0	0	0	0	0	0	0	1
rho_u	0	0	0	0	0	0	0	0	0	0	0	0	0	0	0	0	0	0	0	0	0	1
	-0.1	0	0	0	0	0	0	0	0	0	0	0	0	0	0	0	0	0	0	0	0	1
	-0.2	0	0	0	0	0	0	0	0	0	0	0	0	0	0	0	0	0	0	0	0	1
	-0.3	0	0	0	0	0	0	0	0	0	0	0	0	0	0	0	0	0	0	0	0	1
	-0.4	0	0	0	0	0	0	0	0	0	0	0	0	0	0	0	0	0	0	0	0	1
	-0.5	0	0	0	0	0	0	0	0	0	0	0	0	0	0	0	0	0	0	0	0	1
	-0.6	0	0	0	0	0	0	0	0	0	0	0	0	0	0	0	0	0	0	0	0	1
	-0.7	0	0	0	0	0	0	0	0	0	0	0	0	0	0	0	0	0	0	0	0	1
	-0.8	0	0	0	0	0	0	0	0	0	0	0	0	0	0	0	0	0	0	0	0	1
	-0.9	0	0	0	0	0	0	0	0	0	0	0	0	0	0	0	0	0	0	0	0	1
	-1	1	1	1	1	1	1	1	1	1	1	1	1	1	1	1	1	1	1	1	1	1
	z/y	0	0.0414	0.0828	0.1243	0.1657	0.2071	0.2485	0.2899	0.3314	0.3728	0.4142	0.4556	0.4971	0.5385	0.5799	0.6213	0.6627	0.7042	0.7456	0.787	0.8284
rho_l		0	0	0	0	0	0	0	0	0	0	0										

Fig.2 Computational cells for density around the cross-section of a delta wing in a spreadsheet

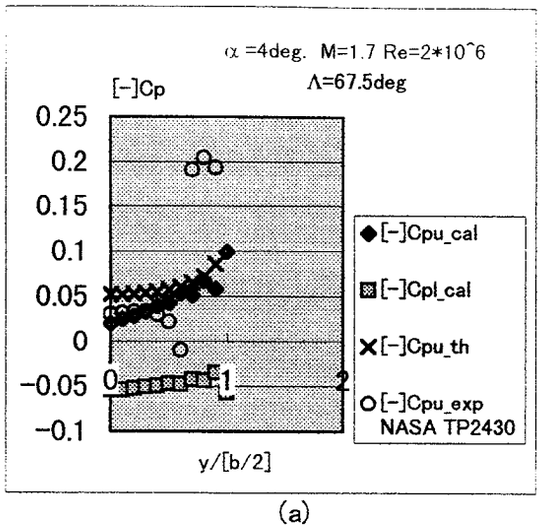

(a)

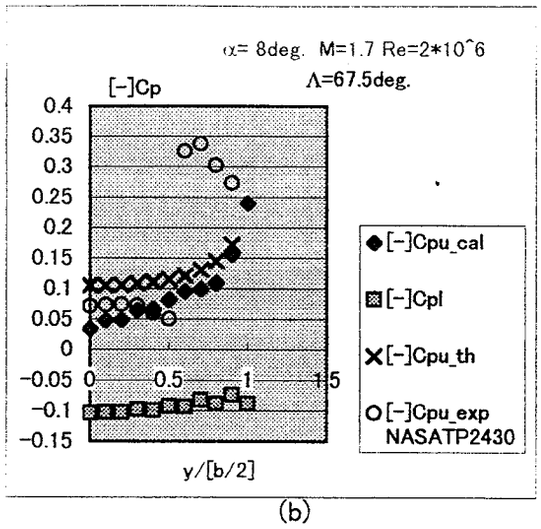

(b)

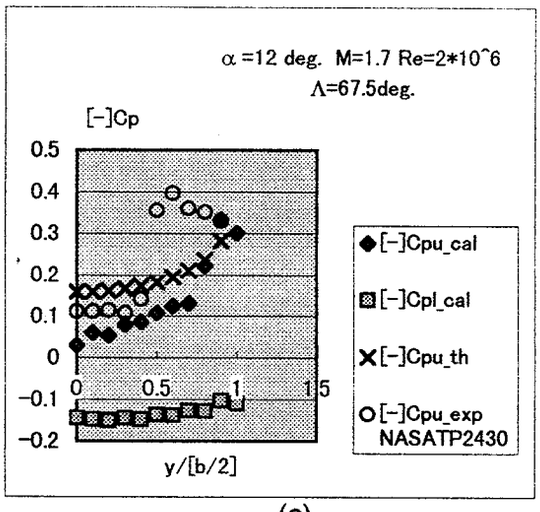

(c)

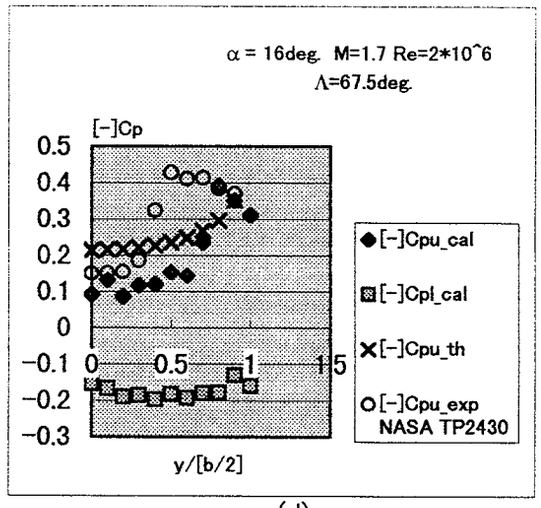

(d)

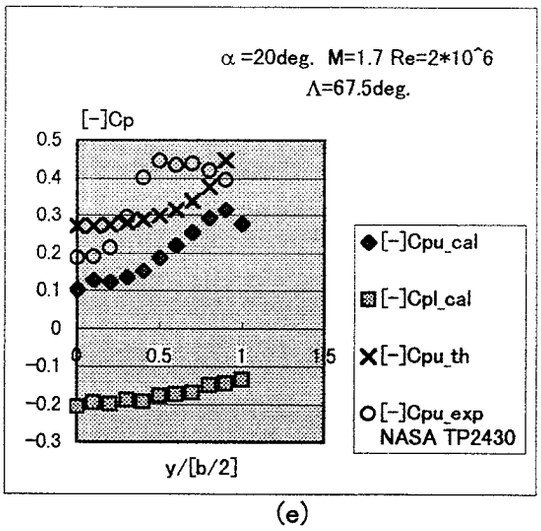

(e)

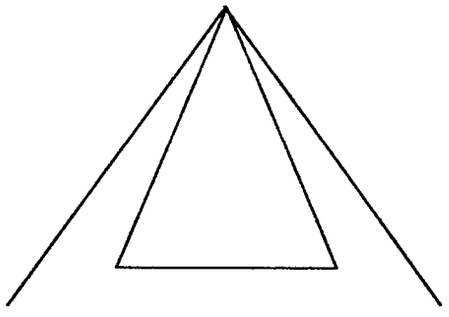

Fig.3 Computational results compared to NASA experiment [Lambda=67.5deg. M=1.7]

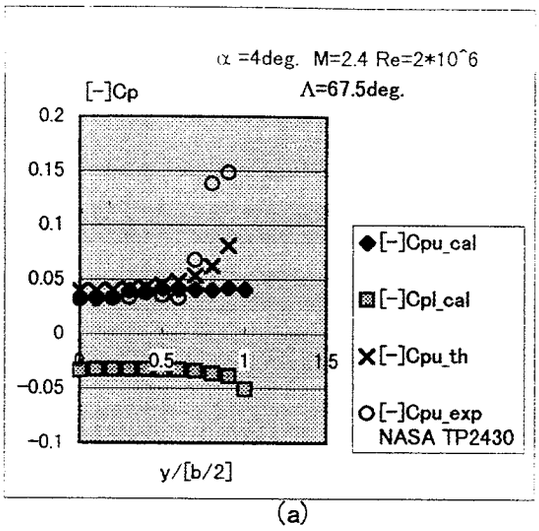

(a)

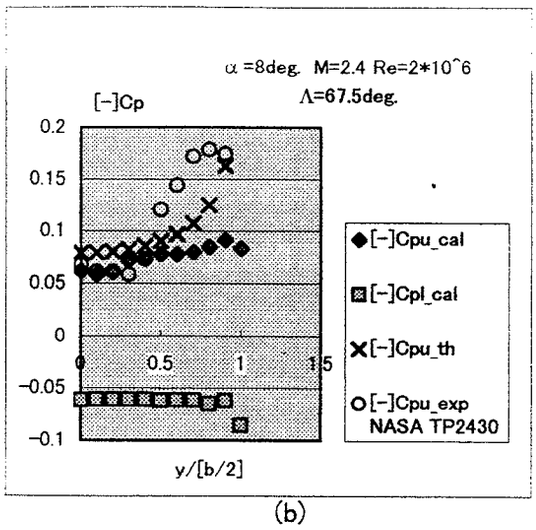

(b)

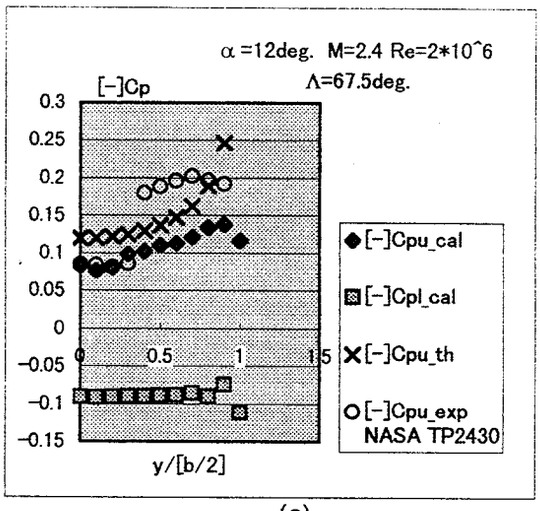

(c)

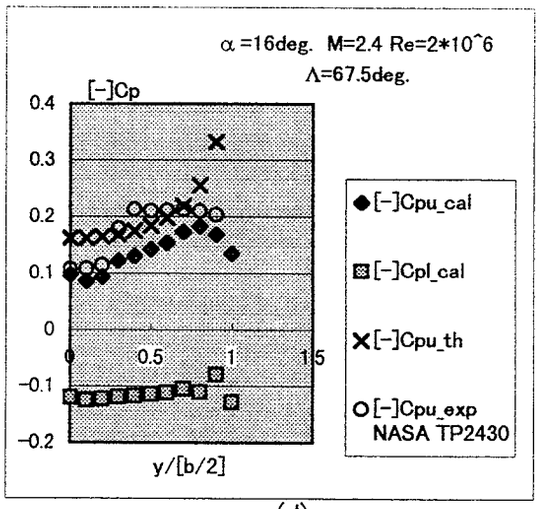

(d)

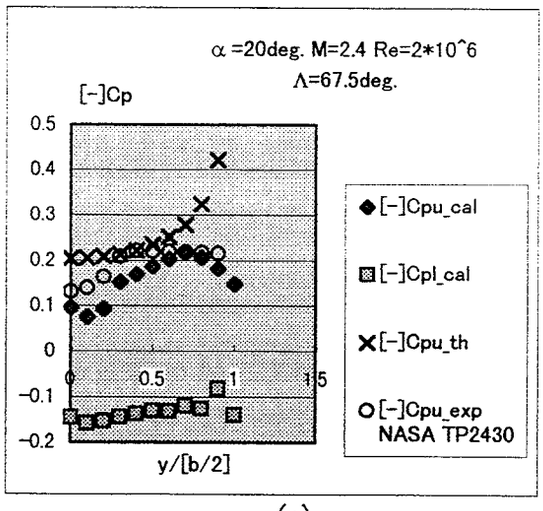

(e)

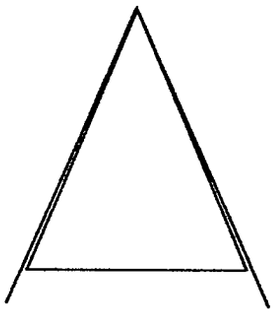

Fig.4 Computational results compared to NASA experiment [Lambda=67.5deg. M=2.4]

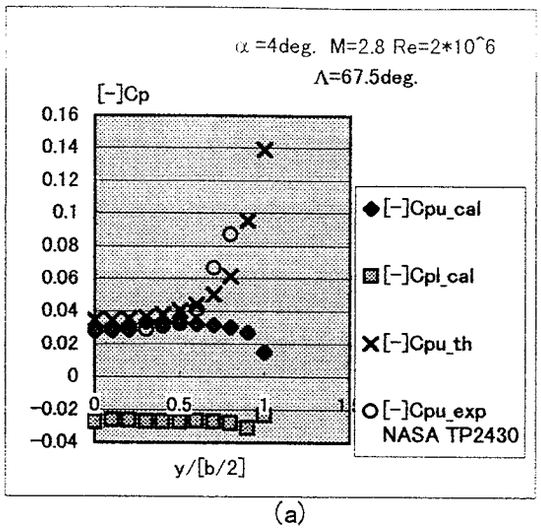

(a)

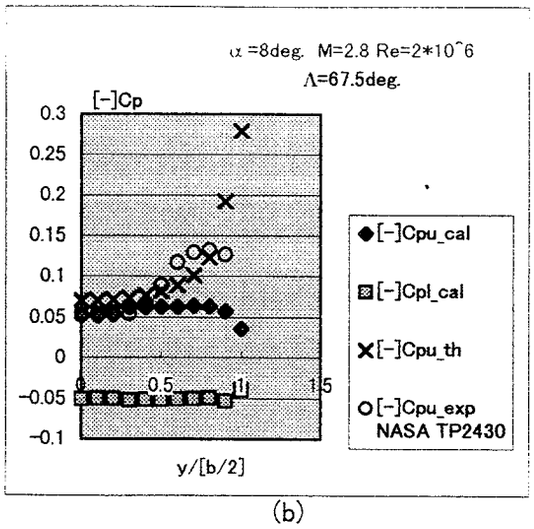

(b)

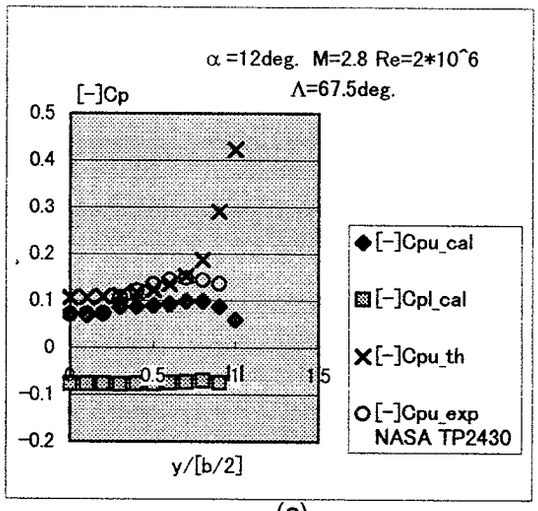

(c)

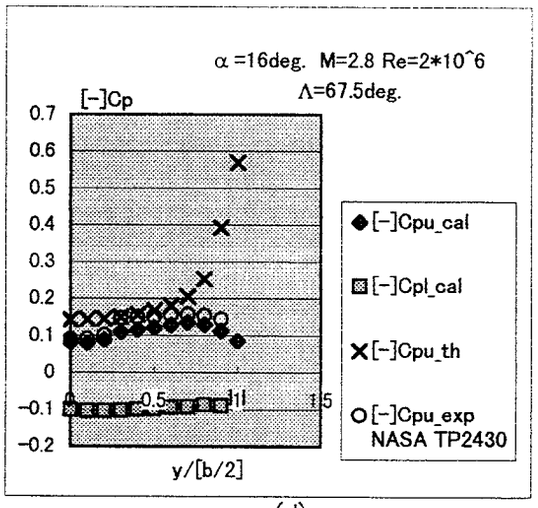

(d)

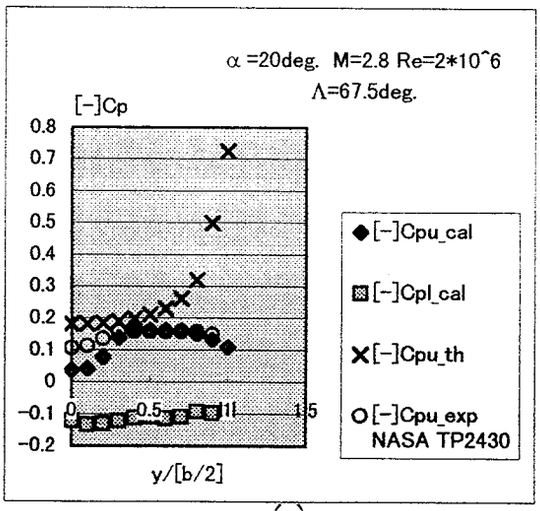

(e)

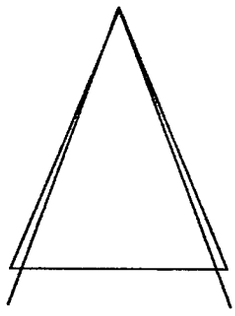

Fig.5 Computational results compared to NASA experiment [Lambda=67.5deg. M=2.8]

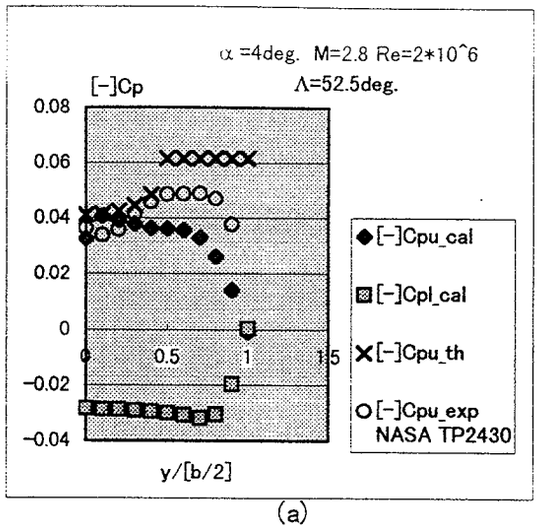

(a)

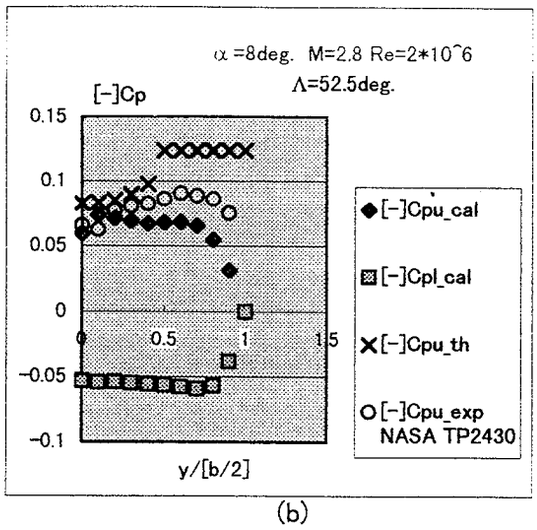

(b)

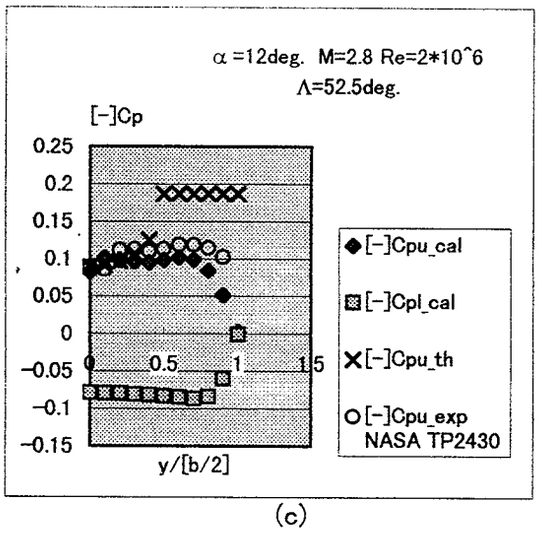

(c)

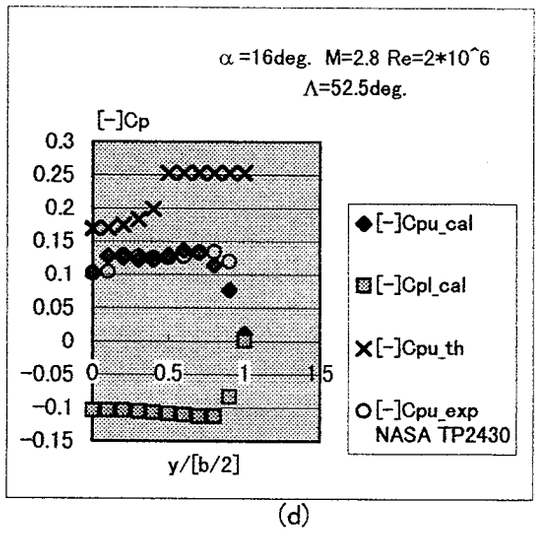

(d)

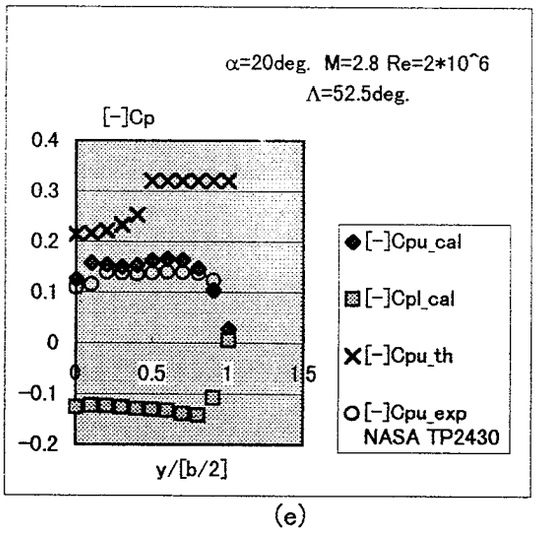

(e)

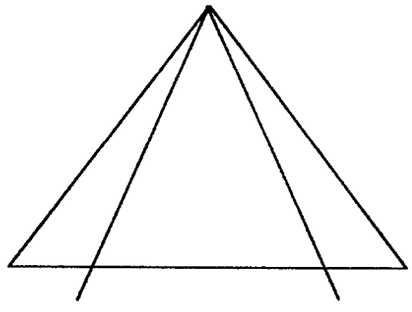

Fig.6 Computational results compared to NASA experiment [Lambda=52.5deg. M=2.8]

190